

THE DEVELOPMENT OF A TOUGH HIGH CHROMIUM FERRITIC STAINLESS STEEL

---

Mavis Ann Hermanus

A Dissertation submitted to the Faculty of Engineering, University  
of the Witwatersrand, Johannesburg in fulfilment of the  
requirements for the Degree of Master of Science in Engineering.

Department of Metallurgy  
University of the Witwatersrand  
March 1986

DECLARATION

I declare that this dissertation is my own, unaided work. It is being submitted for the degree of Master of Science in Engineering at the University of the Witwatersrand, Johannesburg. It has not been submitted before for any degree or examination in any other university.

Mavis Ann Hermanus

MAVIS ANN HERMANUS

11<sup>th</sup> day of April, 1986

ABSTRACTTHE DEVELOPMENT OF A TOUGH HIGH CHROMIUM FERRITIC STAINLESS STEEL

High chromium ferritic stainless steels are very resistant to stress-corrosion cracking and also have good general corrosion and pitting resistance properties. However, they have few applications as materials of construction because they are extremely prone to embrittlement.

The objective of the current project was to develop a tough Fe-40Cr stainless steel. The experimental programme involved an investigation into the effects of interstitial elements (carbon, nitrogen and oxygen) and rare earth metals on toughness. Several experimental alloys were prepared. The interstitial contents ranged from 380 to 840ppm and the rare earth metal additions from 0.05 to 0.9 weight %. The toughness of the alloys was assessed using Charpy impact and slow bend tests. Techniques with which the microstructures were examined and analysed included scanning electron microscopy, transmission electron microscopy and image analysis.

It was shown that tough Fe-40Cr alloys can be produced when suitable heat treatment and processing conditions are employed. Embrittlement was found to be associated with grain boundary precipitation, the extent of which was related to interstitial content and fabrication variables. Finally, rare earth metals proved useful in the development of isotropic toughness properties and the maintenance of toughness at temperatures in excess of 1000°C.

ACKNOWLEDGEMENTS

I am indebted to the following people and institutions for their invaluable advice, use of equipment and, particularly, their encouragement:

Professor Geoff Garrett, Dr John Bee, Dr Pete Wedepohl and Dr Jim Dalton for their interest and enthusiastic supervision of the work.

Members of Mintek, especially my colleague Beth DeMarsh for many useful discussions, and Chris Milward and John Maskrey for their advice and practical assistance.

Members of the Metallurgy Department at the University of the Witwatersrand, especially John Moore, Johnson Ndengeza, Aubrey Xoseke and Yamar Itay for their encouragement and assistance.

Hennie de Klerk at ISCOR for his time and help.

My friends, especially Tony A'Bear and Melinda Silverman for their encouragement, time and help.

Finally, to Mintek, the CSIR and the University of the Witwatersrand for their financial support for the duration of my work.



CONTENTS

	Page
1 <u>INTRODUCTION</u>	1
2 <u>LITERATURE SURVEY</u>	3
2.1 THE PHYSICAL METALLURGY OF FERRITIC STAINLESS STEELS	3
2.1.1 Structure and composition	3
2.1.1.1 Effect of carbon and nitrogen	4
2.1.2 Toughness of ferritic stainless steels	6
2.1.2.1 BCC behavior of Fe-Cr alloys	6
2.1.3 Theory of brittle fracture	11
2.1.3.1 Dislocation theories of brittle fracture initiation	11
2.1.4 Embrittling phenomena in ferritic stainless steels	16
2.1.4.1 Second phase effects inherent in the Fe-Cr system	16
2.1.5 The role of interstitials in embrittlement	24
2.1.5.1 Interstitial precipitates: carbides, nitrides and oxides.	24
2.1.5.2 Austenite and martensite	43
2.1.6 Other factors which influence the DBTT	43
2.1.6.1 Stress state	43
2.1.6.2 Grain size	44
2.1.6.3 Cold work	45
2.1.6.4 Notch sensitivity	45
2.1.7 The relationship between corrosion resistance and embrittlement	47
2.2 THE RHENIUM DUCTILISING EFFECT	52
2.3 RARE EARTH METAL ADDITIONS	58
2.3.1 Chromium and chromium alloys	58
2.3.2 Low alloy steels	61
2.3.3 REM additions in ladle metallurgy	62
2.4 CONCLUDING REMARKS	63

	Page
3 <u>EXPERIMENTAL PROCEDURE</u>	65
3.1 ALLOY PREPARATION	65
3.1.1 The base materials	65
3.1.2 The experimental alloys	65
3.1.3 The melt procedure	66
3.2 THE ADDITION OF RARE EARTH METALS	68
3.3 ROLLING	68
3.3.1 Determination of a fabrication route	69
3.3.2 Rolling of heats V2 and V3	69
3.3.3 Rolling of heat V4	70
3.4 HEAT TREATMENT	71
3.5 MECHANICAL TEST SPECIMEN PREPARATION AND TESTING	73
3.5.1 Charpy impact tests	73
3.5.2 Slow bend tests	74
3.5.3 Tensile tests	78
3.5.4 Hardness tests	78
3.6 MICROSCOPY	79
3.6.1 Optical Microscopy	79
3.6.2 Scanning electron microscopy (SEM)	79
3.6.3 Transmission electron microscopy	80
3.6.4 Microprobe	80
3.7 IMAGE ANALYSIS	81
4 RESULTS AND PRELIMINARY DISCUSSION	82
4.1 RARE EARTH METAL YIELDS	82
4.2 CHARPY TESTS	83
4.2.1 Fabrication route alloys	83
4.2.2 Alloys V2 and V3	84
4.2.3 The V4 alloys	89
4.3 SLOW BEND TESTS	92
4.3.1 Comparison between the Charpy and slow bend results.	97
4.4 TENSILE TESTS	98
4.4.1 The V2 and V3 alloys	98
4.4.2 The V4/0,10 alloy	100

	Page
4.4 HARDNESS TESTS	100
4.4.1 The V1 alloys	100
4.4.2 The V2 and V3 alloys	101
4.4.3 The V4 alloys	102
4.5 OPTICAL METALLOGRAPHY	105
4.5.1 Grain size	105
4.5.2 Interstitial precipitation	106
4.5.2.1 Alloys which do not contain REM	106
4.5.2.2 Alloys which contain REM	107
4.5.3 Sigma precipitation	111
4.5.4 Carbide precipitation	115
4.5.5 Slip mode and fracture initiation studies	115
4.6 SCANNING ELECTRON MICROSCOPY	119
4.6.1 The V2 and V3 alloys	119
4.6.2 The V4 alloys	119
4.6.3 Energy dispersive spectrometry (EDS) in the SEM	125
4.7 ELECTRON MICROPROBE ANALYSIS	128
4.7.1 Alloy V4/0	128
4.7.2 The REM-containing V4/0,1 alloy	132
4.7.3 Alloy V2/1/2	134
4.7.4 Summary	134
4.8 TRANSMISSION ELECTRON MICROSCOPY	136
4.9 IMAGE ANALYSIS	137
4.9.1 The effect of different annealing temperatures	141
4.9.2 The effect of different interstitial element contents	144
4.9.3 The effect of REM additions	149
4.9.4 Summary	151
5 DISCUSSION	152
5.1 MECHANICAL TEST RESULTS	152
5.1.1 Comparison between the impact energies obtained in the current study and those quoted in the literature.	152
5.1.2 Discrepancies between the Charpy and slow bend test results.	154
5.1.3 Scatter in the impact and slow bend test results.	156



	Page
5.1.4 The effects of interstitial impurity levels, grain size and REM content on the tensile properties of Fe-40Cr	157
5.2 THE EFFECTS OF COMPOSITION, HEAT TREATMENT AND FABRICATION PARAMETERS ON TOUGHNESS	161
5.2.1 The alloys containing no REM	161
5.2.2 REM-containing alloys	163
5.2.3 The relationship of the nominal composition of the Fe-40Cr to toughness	165
5.3 MICROSTRUCTURE AND IMPACT TOUGHNESS PROPERTIES	167
5.3.1 Grain size	167
5.3.2 Carbide and $\sigma$ -phase precipitation	168
5.3.3 General theory of brittle fracture	168
5.4 SUMMARY	173
5.4.1 Fabrication procedure	173
5.4.2 Embrittlement	173
5.4.3 The effect of REM additions on toughness properties	174
5.4.4 Fractography	174
5.4.5 Grain size effects	174
5.4.6 Interstitial levels	175
5.4.7 The nominal composition	175
6 <u>CONCLUSIONS AND RECOMMENDATIONS FOR FUTURE WORK</u>	176
6.1 CONCLUSIONS	176
6.2 RECOMMENDATIONS FOR FUTURE WORK	176
6.2.1 Economic survey	177
6.3.1 Laboratory work	177
REFERENCES	179
APPENDICES	189
A: Computer programs (slow bend tests)	190
B: Slow bend tests	191
C: Computer programs for image analysis	199



1 INTRODUCTION

Ferritic stainless steels were developed in Europe over 70 years ago<sup>1</sup>. They are iron-based alloys containing at least 11% chromium. The upper limit of the chromium content is arbitrary, although commercially-produced alloys contain a maximum of 35% chromium at present<sup>2</sup>.

Although ferritic stainless steels, especially those with higher chromium contents, have excellent corrosion resistance in many environments and are not susceptible to stress corrosion, their use has been extremely limited in comparison to austenitic stainless steels due to their marked tendency to embrittlement. Loss of ductility can be attributed to a number of causes such as the presence of interstitial elements such as carbon and nitrogen. For example, a 25% chromium steel will be brittle at room temperature if the carbon content exceeds 0.03%<sup>3</sup>. Another factor is the absence of a phase change which makes it difficult to refine the ferrite grain size. The grain size can become very coarse after high temperature heat treatments and welding. In addition solid state reactions which are inherent in the Fe-Cr system, can produce brittle intermetallic phases.

Despite these limitations, metallurgical interest in these alloys continues because of their excellent resistance to stress corrosion cracking and oxidation, and the high cost of nickel needed to stabilise the austenite in austenitic stainless steels<sup>1,2,4,5</sup>. Intensive research over the past two decades and recent advances in commercial steel-refining practice has shown that tough, ductile ferritic stainless steels containing up to 35% chromium can be produced when interstitial contents are reduced to very low levels. Tough chromium alloys can also be obtained by alloying with small amounts (up to 0.7%) of rare earth metals (La, Ce etc.) and certain elements such as Ta which are strong carbide-formers.

These developments have resulted in the production of ferritic

alloy compositions which are fabricable and weldable - the so called 'super ferritic' stainless steels. Although these steels are tougher than their predecessors, they remain susceptible to catastrophic failure. Consequently, the mechanisms of brittle fracture in ferritic stainless steels remain an important area of research.

The purpose of the current project was to investigate specifically the influence of interstitial concentration and rare earth metal (REM) additions on the structure and properties of an Fe-40Cr alloy. The literature survey therefore concentrated on prior work directly relating to the study in the areas of ferritic stainless steels, the ductilizing effect and the benefits of REM additions. The experimental work included Charpy, slow bend and tensile tests. Various techniques, such as optical and scanning electron microscopy, and image analysis were also used in the investigation.

2

LITERATURE SURVEY

The literature survey is divided into three parts. Each part highlights a particular aspect important to the development of viable high chromium alloys. Part one, the most extensive, focusses on the problems related to interstitial impurities, part two explores the relationship between phase relations, composition and properties in binary alloys and part three describes the influence of rare earth elements on the properties of steels in general.

2.1 THE PHYSICAL METALLURGY OF FERRITIC STAINLESS STEELS

2.1.1 Structure and composition

In theory the structure of ferritic stainless steels is simple. The addition of chromium to iron restricts the formation of the face-centred cubic (FCC) austenite phase while the ferritic body-centred cubic (BCC) phase is stabilised. This results in a closed austenite ( $\gamma$ ) loop in the iron-chromium system as shown in Figure 2.1.

At all temperatures binary iron-chromium alloys which contain more than 13% chromium are thus essentially ferritic and consist of a chromium-iron alpha ( $\alpha$ ) solid solution.

Two other phases viz. sigma ( $\sigma$ ) and alpha-prime ( $\alpha'$ ) are integral to the Fe-Cr system. Sigma is a tetragonal intermetallic phase with an approximate composition of  $\text{FeCr}^{1.7}$ . As shown in Figure 2.1, it occurs in alloys containing between 15 and 70% chromium which have been exposed to temperatures from about 500 to 800°C. Alpha-prime ( $\alpha'$ ) forms when a ferritic iron-chromium stainless steel is heated at temperatures between 400 and 540°C. In this temperature range the ferrite solid solution separates into iron-rich ( $\alpha$ ) and chromium-rich ( $\alpha'$ ) fractions. This phenomenon is often referred to as 475°C embrittlement. The embrittlement associated with the  $\sigma$  and  $\alpha'$  phases is discussed later (in Section 2.1.4).



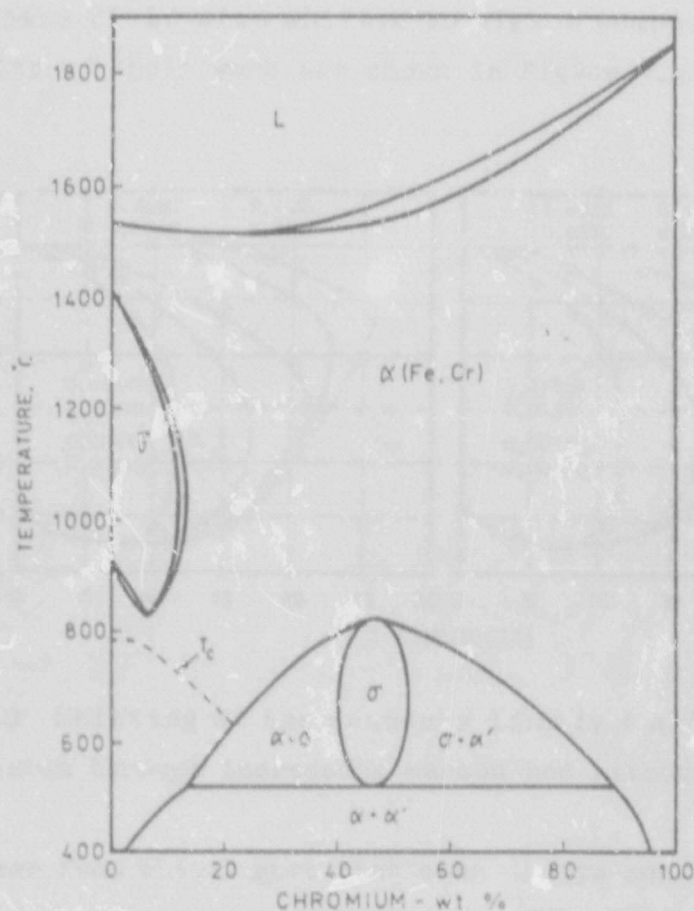


Figure 2.1 The Fe-Cr system<sup>2</sup>

#### 2.1.1.1 The effect of carbon and nitrogen

Commercial ferritic stainless steels always contain small amounts of carbon and nitrogen and cannot be strictly described as binary Fe-Cr alloys. Most often, carbon is a residual element which is not completely removed from the raw materials during refining, while nitrogen is introduced into the alloy by contact with air during melting<sup>2</sup>.

Both carbon and nitrogen are potent austenite-stabilising elements and push the outside boundary of the ( $\gamma + \alpha$ ) two phase field to higher chromium levels. Baerleken, Fisher and Lorenz<sup>6</sup> have studied the effects of carbon and nitrogen on the location of the  $\gamma$ -loop in the iron-chromium phase diagram. They noted that as the carbon and nitrogen content increased, the two-phase region not only shifted to higher chromium levels but the maximum extension of the



( $\gamma + \alpha$ ) phase field also shifted to higher temperatures. Some of the results of their work are shown in Figure 2.2.

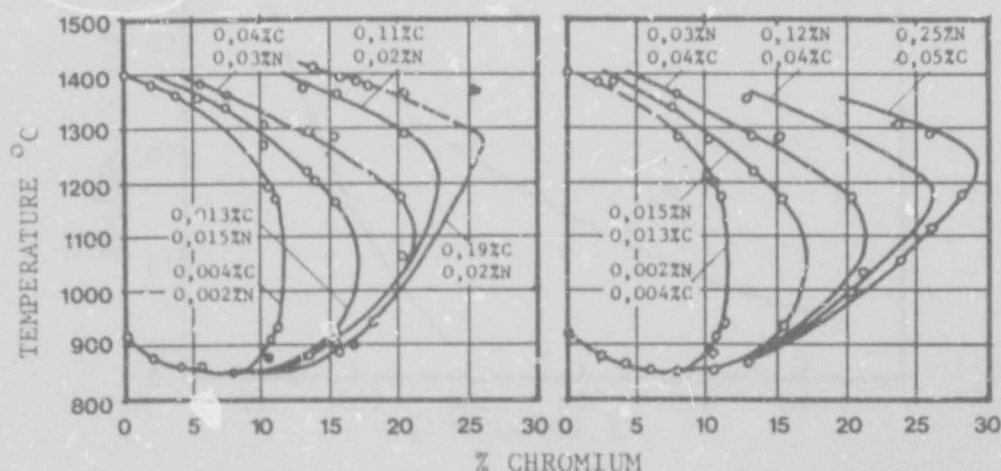


Figure 2.2 Shifting of the boundary line ( $\gamma + \alpha$ )/ $\alpha$  in the system iron-chromium through increasing carbon and nitrogen contents<sup>6</sup>.

It is clear from this figure that even alloys containing more than 25% Cr, will undergo a phase transformation if sufficient quantities of carbon and nitrogen are present. Thus welded, and some annealed, ferritic stainless steels can contain austenite and untempered martensite. The effects of these phases on properties are discussed in Section 2.1.5.2.

In addition to extending the region of austenite stability, carbon and nitrogen also form precipitates during cooling since their solid solubility in the matrix decreases with decreasing temperature. The solubility of carbon and nitrogen in an Fe-26%Cr alloy as a function of temperature is shown in Figure 2.3.

In chromium-containing alloys, carbon generally forms the complex carbides  $(\text{Cr,Fe})_7\text{C}_3$  and  $(\text{Cr,Fe})_{23}\text{C}_6$  which precipitate on the grain boundaries<sup>2,4</sup>, while nitrogen generally precipitates as intragranular  $(\text{CrFe})_2\text{N}$  precipitates<sup>2</sup>. This carbide and nitride precipitation can result in severe embrittlement of Fe-Cr alloys, (see Section 2.1.5).

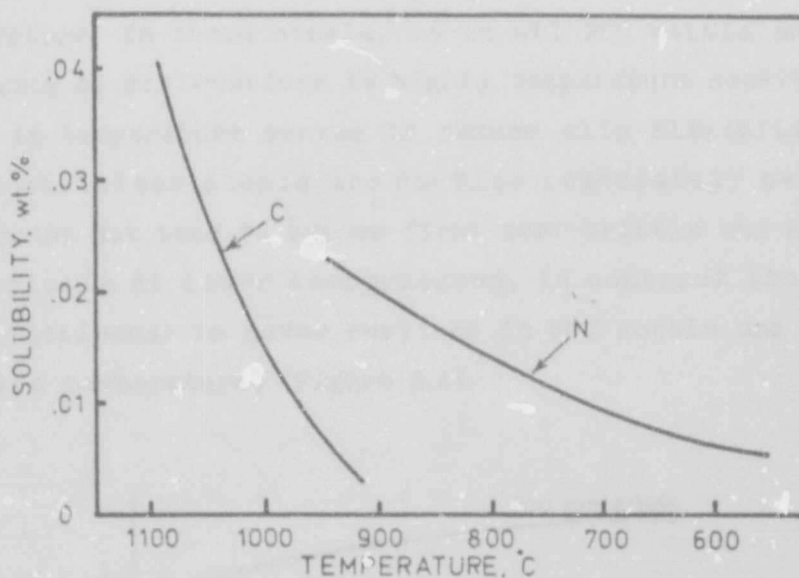


Figure 2.3 Solubility of C and N in the Fe-26% Cr<sup>2</sup>.

#### 2.1.2 Toughness of ferritic stainless steels

All BCC metals and alloys show a ductile-to-brittle-transition-temperature (DBTT). At low temperatures, the fracture mechanism is brittle cleavage while at higher temperatures fracture occurs by ductile tearing. In ferritic stainless steels, the principle limitation is a relatively high DBTT. Thus their low toughness, even at ambient temperatures, can lead to catastrophic failure of engineering structures.

The DBTT is affected by a number of factors, such as the thermal history of the alloy, alloying elements, grain size, secondary phases, segregation, strain rate and the prevailing stress system<sup>1,2,7</sup>. Before discussing these, attention is focussed on the BCC behavior of the alloys and theories of brittle fracture.

##### 2.1.2.1 BCC behavior of Fe-Cr alloys

Much of the problem with the toughness of ferritic stainless steels is related to the fact that the crystal structure is BCC<sup>8</sup> and although there are many variables associated with the

transition from a non-brittle to brittle state, the most important is temperature. In these steels, as in all BCC metals and alloys, the mobility of dislocations is highly temperature sensitive and a decrease in temperature serves to reduce slip flexibility<sup>9</sup>. Thus ferritic stainless steels are ductile immediately below their melting point but tend to become first semi-brittle and ultimately highly brittle at lower temperatures. In contrast the tendency towards brittleness is never realised in FCC metals and alloys at reasonable temperatures (Figure 2.4).

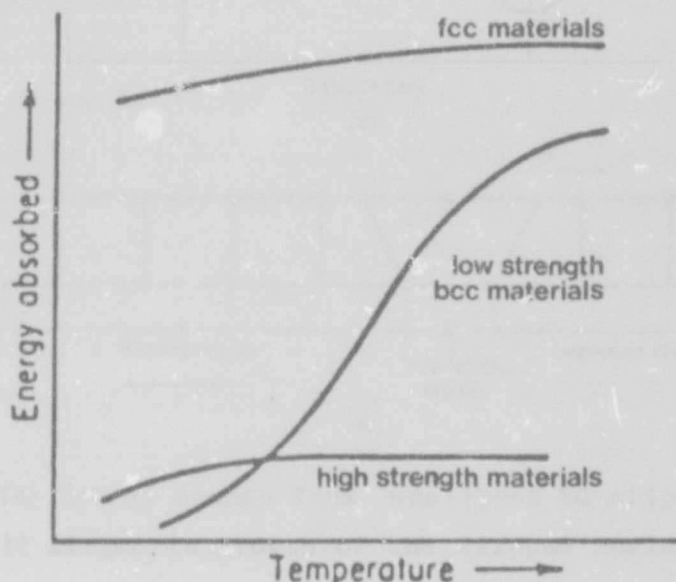
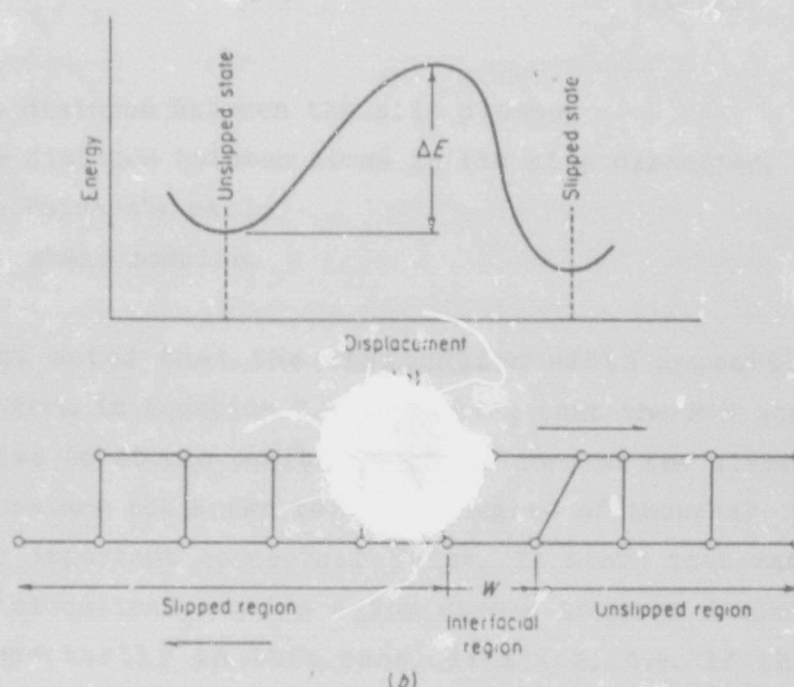


Figure 2.4 Effect of temperature on notch toughness (schematic)<sup>10</sup>.

The relationship between toughness and temperature in BCC metals can be explained in terms of Cottrell's model of slip by dislocation motion<sup>9</sup>. This considers that plastic deformation is the transition of material from an unslipped to a slipped state, i.e. plastic deformation involves slip. In a perfect lattice all the atoms above and below a slip plane are in a minimum energy position. In order for plastic deformation to occur, an atom has to be shifted from its initial low energy position to a new one. The process is opposed by an energy barrier,  $E$ , which corresponds to the atom in the high energy transitional state (Figure 2.5a).



All atoms in a slip plane do not move simultaneously. To minimise the energy of the process the slipped region grows at the expense of the unslipped region by the advance of an interfacial area (Figure 2.5b).



**Figure 2.5** (a) Energy change from unslipped to slipped state:  
(b) stages in growth of the slipped region<sup>10</sup>.

The interfacial area is a dislocation. To minimise the energy for the transition, the interface thickness,  $w$ , should be as narrow as possible. The dimension,  $w$ , in Figure 2.5b is the width of the dislocation, and is related to the elastic energy of the crystal. When the elastic energy of the crystal is low the dislocation is wide and the atomic spacing in the slip direction is closer to its equilibrium spacing. The opposing energy changes, elastic energy and transition energy, determine the equilibrium width of the dislocation.

The dislocation width is important because it determines the magnitude of the force required to move a dislocation through the crystal lattice. This force is called the Peierls-Nabarro force, while the Peierls-Nabarro (P-N) stress is the shear stress



required to move a dislocation through a crystal lattice in a particular direction.

The Peierls-Nabarro stress, is given by:

$$\left(\frac{2G}{1-\nu}\right)e^{-2\pi w/b} \approx \left(\frac{2G}{1-\nu}\right)e^{-[2\pi a/(1-\nu)b]} \quad \dots\dots 2.1$$

where     $a$  = distance between the slip planes,  
           $b$  = distance between atoms in the slip direction,  
           $\nu$  = Poisson's ratio,  
           $G$  = shear modulus.

It should be noted that the dislocation width appears in the exponential term in Equation 2.1 indicating that the P-N stress is very sensitive to atomic positions at the core of the dislocation. Although these are not known to a high degree of accuracy, the P-N equation has important conceptual value. It shows that materials with wide dislocations require a low stress to move dislocations and more importantly in this case, if  $a < b$ , i.e. if the slip planes are closely spaced but loosely packed, the P-N stress is high. The slip planes in BCC metals approach this situation, whereas in FCC structures there are many close-packed slip systems available. BCC metals are thus brittle at low temperatures because thermal energy is no longer available to help them to overcome the higher barrier which is associated with their structure. The dislocations in these materials are then effectively immobilised<sup>9,10,11</sup>.

Although the occurrence of the DBTT in ferritic stainless steels can be explained in terms of crystal structure, the reasons for the ductile-to-brittle-transition in temperature ranges of engineering interest are essentially related to the sensitivity of this structure to even the smallest levels of interstitial impurities. This is illustrated by the fact that zone-refined BCC polycrystals can be ductile at temperatures as low as  $-269^{\circ}\text{C}$ <sup>8</sup>.

Loomis and Carlson<sup>12</sup> suggested that interstitials in solid solution are progressively embrittling and in the group VIIa metals they can be ranked in order of importance as hydrogen, oxygen, nitrogen and carbon. These atoms distort the lattice strongly but are very mobile in ferrite. However, at relatively low temperatures they are attracted to both edge and screw dislocations where they can fit with less elastic strain.

The binding energy of a solute atom and a dislocation is about 0.5eV and because the distorted lattice is tetragonal and contains a large component of shear strain, the solute atoms interact strongly with edge dislocations through lattice expansion, as well as with screw dislocations through their shear stress field. Thus the conditions for the segregation of all solute atoms to dislocations is exceptionally favourable in BCC iron. The dislocations are immobilised by the strong pinning effect of the atoms segregated to them and the density of dislocations available for glide is reduced to virtually zero unless stresses are applied which are sufficiently high to release the pinned dislocations or to create new ones from points of stress concentration<sup>11</sup>. Under these conditions the applied stresses may well result in brittle fracture rather than plastic deformation. In this way brittle fracture at ambient and higher temperatures is possible.

Because the solubility levels of interstitials in ferritic stainless steels is so low, and the presence of carbon, nitrogen and oxygen beyond their solubility limits also increases the DBTT, it is rarely possible to separate solute effects from the effects of carbide, nitride and oxide precipitation. These precipitates may:

- (i) inhibit slip propagation across the grain boundaries,
- (ii) crack and lead to crack propagation in the adjacent matrix:  
and/or
- (iii) inhibit dislocation motion within the grains<sup>8</sup>.

These effects of the interstitial solutes are discussed in Section 2.1.5.

### 2.1.3 Theory of brittle fracture

The toughness of ferritic stainless steels is generally assessed in terms of a DBTT. This temperature is not constant and an understanding of factors affecting it and the theory of brittle behaviour is essential if the effects of metallurgical variables on the fracture process are to be understood. Ultimately appropriate manipulations of these variables should result in the development of steels with adequate toughness.

A number of theories have been formulated to explain the mechanisms of the nucleation of brittle fracture on the basis of dislocation movement. Two of them, due to Stroh<sup>13</sup> and Cottrell<sup>7,14</sup> are examined here.

#### 2.1.3.1 Dislocation theories of brittle fracture initiation

Zener<sup>15</sup> first advanced the idea that high stresses at the head of a dislocation pile-up can produce fracture. The shear stress acting on the slip plane squeezes the dislocations together. At some critical value of stress the dislocations at the head of the pile-up are forced so close together that they coalesce into a wedge crack or cavity dislocation of height,  $nb$  and length,  $2c$  (Figure 2.6).

Stroh<sup>13</sup> analysed this situation and showed that, provided the stress concentration at the head of the pile-up is not relieved by plastic deformation, the tensile stress at the pile-up is given by:

$$\frac{3}{2} \left( \frac{L}{r} \right)^{1/2} \tau \sin \theta \cos \frac{\theta}{2} \quad \dots\dots\dots 2.2$$

where  $\tau$  = average resolved applied shear stress,  
 $L$  = length of the blocked slip band, and  
 $r$  = distance from the tip of the pile-up to the point  
where the crack is forming.



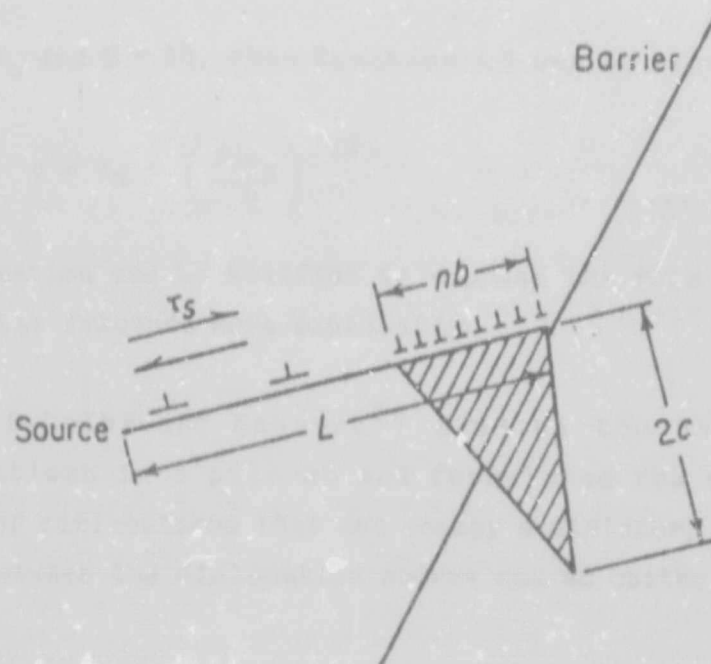


Figure 2.6 Model of microcrack formation at a pile-up of edge dislocations<sup>10</sup>.

This can be equated to the theoretical cohesive stress<sup>8</sup>,  $\sigma_{max}$ , where

$$\sigma_{max} = \left( \frac{E\gamma_s}{a_0} \right)^{1/2} \quad \text{.....2.3}$$

Thus, the condition for microcrack nucleation is:

$$(\tau - \tau_0) \frac{L}{b}^{1/2} \geq \left( \frac{E\gamma_s}{a_0} \right)^{1/2} \quad \text{.....2.4}$$

where  $\tau_0$  = resistance of the lattice to dislocation movement,

$a_0$  = equilibrium spacing between planes of atoms,

$E$  = Youngs modulus, and

$\gamma_s$  = specific surface energy of the implied crack.

The applied stress required to initiate cleavage is:

$$\tau = \tau_0 + \left( \frac{E\gamma_s}{La_0} \right)^{1/2} \quad \text{.....2.5}$$



If  $r = a_0$  and  $E = 2G$ , then Equation 2.5 can be expressed as:

$$\tau = \tau_0 + \left( \frac{2G\gamma_s}{L} \right)^{1/2} \dots\dots\dots 2.6$$

This equation can be modified to express the role of dislocations in brittle fracture more explicitly.

Frank, Eshelby and Nabarro<sup>16</sup> studied the distribution of dislocations in a pile-up and formulated the theory that the number of dislocations that can occupy a distance,  $L$ , along a slip plane between the dislocation source and an obstacle is given by:

$$n = \frac{k\pi L}{Gb} \dots\dots\dots 2.7$$

where  $k$  = a factor close to unity (for an edge dislocation,  $k = (1 - \nu)$ , where  $\nu$  = Poisson's ratio, while for a screw dislocation,  $k = 1$ , and  $b$  = unit Burger's vector

This theory was experimentally confirmed by Meakin and Wilsdorf<sup>17</sup>.

It has also been shown<sup>18</sup> that the number of dislocations in a slip band can be expressed as:

$$nb \approx L \left( \frac{\tau - \tau_0}{G} \right) \dots\dots\dots 2.8$$

and, when  $L$  is eliminated from equation 2.5 and 2.8, the following expression is obtained:

$$(\tau - \tau_0)nb \approx 2\gamma_s \dots\dots\dots 2.9$$

This equation has the direct physical significance that a crack will form when the work done by the applied stress in producing a displacement,  $nb$ , equals the work done in moving dislocations against the friction stress plus the work done in producing new

surfaces. The equation for microcrack nucleation was first proposed by Cottrell in this form<sup>10,11</sup>.

Smith and Barnby<sup>10</sup> have shown that the stress required to nucleate a microcrack is significantly lower than that predicted and have modified Stroh's equations to allow for a non-uniform stress field and dislocations of both signs in the existing pile-up.

Further work by Petch<sup>19</sup> accounted for the most difficult step of crack propagation, i.e. propagation through a strong barrier such as a grain boundary. It was found that the dependence of brittle fracture in iron and steel on grain size could be expressed as:

$$\sigma_y = \sigma_0 + k_y d^{-1/2} \quad \dots\dots\dots 2.10$$

where  $\sigma_y$  = flow or fracture stress or both,  
 $\sigma_0$  = lattice friction stress,  
 $k_y$  = Hall-Petch slope, and  
 $d$  = grain size (diameter).

Cottrell then reformulated Equation 2.9 in terms of normal stress so that the important variables in brittle fracture such as grain size can be easily shown:

$$\sigma_{nb} \approx 4\gamma_s \quad \dots\dots\dots 2.11$$

Substituting Equation 2.9 into equation 2.11, we have

$$\sigma(\tau - \tau_0)d = 8\mu\gamma_s \quad \dots\dots\dots 2.12$$

where  $L = d/2$  (i.e. the dislocation source is at the centre of the grain) and  
 $\mu$  = shear modulus.

But experience has shown that microcracks form when the shear stress equals the yield stress and that the observed stresses for yield and fracture are more likely to correspond at larger grain

sizes and at low temperature. Assuming that  $\tau = \sigma/2$  (i.e. shear stress is at maximum), Equation 2.4 can be written as:

$$\tau = \tau_0 + \frac{k_y d^{-1/2}}{2} \quad \dots\dots\dots 2.13$$

And finally equations 2.12 and 2.10 can now be restated as:

$$\sigma_y k_y d^{1/2} = k_y^2 + \sigma_0 k_y d^{1/2} > C \gamma_s \quad \dots\dots\dots 2.14$$

where  $C$  = a constant related to the stress state and average ratio of normal to shear stress on the slip plane.

Although equation 2.14 does not encompass all the practical models of crack initiation, (e.g. nucleation of cleavage cracks at twins or at the boundaries between second phase particles and the matrix of a steel) it nevertheless provides a useful basis for discussing the micro-mechanics of brittle fracture. The equation essentially describes the condition for a brittle-to-ductile transition. When the left hand side of the equation is smaller than the right, a microcrack can form, but cannot grow. Alternatively, if the left hand side of the equation is greater than the right a propagating brittle fracture is produced at a shear stress equal to the yield stress.

Process and compositional variables can directly affect all the factors in this equation<sup>8,9,10,11,20,21,22</sup>. For example:

- $k_y$  is related to the number of dislocations that are released into a pile-up when a source is unlocked and is affected by solute distribution and grain boundary precipitation,
- $d$ , the grain size, is rather related to the slip band length, since in alloys containing fine precipitates the particle spacing rather than the actual grain size will determine the slip distance,
- $\gamma$  is affected by the presence of flaws in the microstructure (e.g. needle-like precipitates lower  $\gamma$ ),



**Author** Hermanus Mavis Ann

**Name of thesis** The development of a tough high chromium ferritic stainless steel. 1986

***PUBLISHER:***

University of the Witwatersrand, Johannesburg

©2013

***LEGAL NOTICES:***

**Copyright Notice:** All materials on the University of the Witwatersrand, Johannesburg Library website are protected by South African copyright law and may not be distributed, transmitted, displayed, or otherwise published in any format, without the prior written permission of the copyright owner.

**Disclaimer and Terms of Use:** Provided that you maintain all copyright and other notices contained therein, you may download material (one machine readable copy and one print copy per page) for your personal and/or educational non-commercial use only.

The University of the Witwatersrand, Johannesburg, is not responsible for any errors or omissions and excludes any and all liability for any errors in or omissions from the information on the Library website.